JOURNAL OF SPACECRAFT AND ROCKETS
Vol. 32, No. 2, March–April 1995

Fast Variable-Amplitude Cold Gas Thruster

William C. Stone*
National Institute of Standards and Technology, Gaithersburg, Maryland 20899

A fast response variable amplitude cold gas thruster is described. A laboratory prototype comprised of a piezoelectric stack and an associated microprocessor-based programmable dc power source, a low-loss mechanical displacement amplifier, a high-pressure spring-loaded axial valve, an integral high-pressure valve seat; an expansion nozzle, and a high-pressure gas supply were constructed and tested. The device is designed to operate as a stand-alone unit with a dedicated onboard microcontroller system and onboard energy storage system. Minimum pulse-width resolution (base-to-base) was shown to be 0.98 ms, with a lag time of 0.37 ms relative to the initiation of the drive pulse. Linear amplitude response was achieved beyond a threshold drive voltage of 80 vdc and was maintained through the limit of testing at 240 vdc.

Nomenclature

C = Capacitance of piezoelectric stack, F
E_{HSILS} = Active energy dissipation in high-speed intelligent loading system drive pulse, J
E_{RCS} = Active energy dissipation in solenoid drive pulse, J
n = Number of data scans
R = Solenoid resistance, ohms
$t(i)$ = Time at data scan i, s
V_{peak} = Maximum drive pulse voltage
$V(i)$ = Drive pulse voltage at scan i

Introduction

A SERIES of mathematical investigations were carried out at the National Institute of Standards and Technology with the objective of developing robust system identification techniques for the response of flexible structures.[1–5]

These techniques are likely to be particularly useful for structural systems with noncollocated active control, where noise is present in the sensor data used as input to the active control algorithm. Examples of such structural systems include flexible robotic manipulators and large orbiting spacecraft.

The research reported in Refs. 1–5 was based on the finding that it is advantageous to recover the dynamic characteristics of a structure by deconvolution of an output caused by an excitation by a pulse defined by an inverse Gaussian function or an approximation thereof. Where identification of higher order mode shapes and frequencies is sought, the drive pulse must be short. In the case of certain spacecraft, for example, it is apparent that active control systems should accommodate structural response at frequencies of vibration of several hundred Hz.[6] This would, in turn, require an actuator to impart to the structure a smooth, unidirectional, mathematically defined test pulse whose total duration is less than 0.001 s, for example.

The advantages of such a device motivated research at the National Institute of Standards and Technology with the goal of developing a working prototype high-speed intelligent loading system, or HSILS[7,8] and to ascertain its pulse-width resolution, its ability to vary amplitude interactively (force applied to the test structure), and the feasibility of generating mathematically definable force-time histories using either closed or semiclosed loop control. Implicit in the latter objective was the necessity of employing an onboard, programmable microprocessor control system that could be used to drive the device as a stand-alone thruster.

In the present paper, the background of the design, the rationale behind the selected technology, and the experimentally observed pulse-width resolution and amplitude control behavior of the system are discussed. Although initially developed for research purposes in system identification, the prototype device described presents the basis for a cold gas, or monopropellant, thruster technology with significantly improved performance characteristics over traditional reaction control system jets.

Received Aug. 17, 1993; revision received Nov. 3, 1993; accepted for publication Nov. 9, 1993.

*Research Engineer, Structures Division, Bldg. 226/B168. Member AIAA.

Mechanical Development

The heart of most reaction control system technologies resides in an internal valve mechanism. A slow valve results in a thruster with slow response, no matter how optimized the control electronics may be. An extensive background study of valves and fast mechanism technology was conducted that included servo-hydraulics and servo-pneumatics, solenoids, piezoelectric-pumped systems, and various related designs used for injection of trace elements into spectrophotometers, fuel injectors, electrical relays and dot matrix printer actuators.[9] On the basis of these studies it was decided to proceed with the development of a fast valve that employed a piezoelectric actuator combined with mechanical displacement amplification.

Briefly, the thruster incorporates a very high speed, electronically controllable valve system capable of continuously metering the flow of pressurized gas and/or pressurized propellants through an expansion nozzle to create thrust. The device may be envisioned in a simplified way as shown in Figs. 1–3, in which a valve core element seats directly against the throat of an expansion nozzle. Axial (vertical) displacement of the valve core, under the command of an embedded microcontroller (Fig. 4), causes a gap to form that permits mass flow from the pressurized fuel container to the expansion nozzle. As long as the annular area determined by the gap between the valve core and the valve seat remains less than the nozzle throat area, linear thrust control is possible. Because maximum thrust is directly proportional to nozzle throat diameter, the device can be scaled to achieve desired peak thrust levels in a straight forward manner. Although the prototype was designed as a cold gas thruster, the extension of the technology described below to monopropellant and hypergolic bipropellant thrusters is obvious.

The heart of the high-speed valve is a monolithic (or "co-fired") piezoelectric (or electrostrictive) stack. A custom PZT stack measuring 76 mm long by 9.5 mm square was produced especially for the project. This stack was capable of producing 0.2% strain when subjected to an electic potential of approximately 300 volts, dc. This strain is essentially fully developed within 10 μs of the application of a step change in voltage to the stack, and therefore allows for extremely rapid displacement control, provided an appropriate voltage-time history can be applied to the stack. Electrostrictive characteristics, including blocked force response, of this piezoelectric stack are presented in Fig. 5. A blocked force response chart shows the relationship between the maximum force level capable of being developed by the piezoelectric element between a pair of rigid reaction surfaces at a specified level of total expansion when the element is driven at a constant voltage. There exists a family of

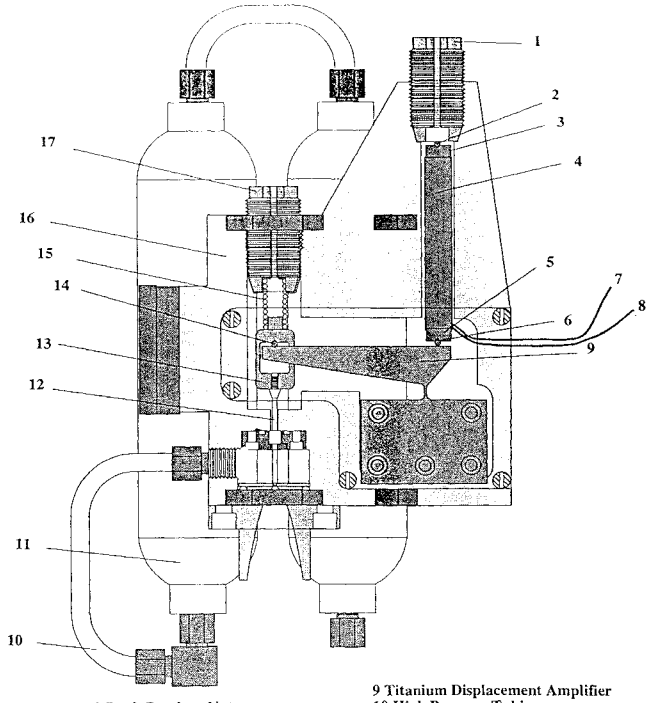

Fig. 1 Side view of HSILS showing all internal moving components.

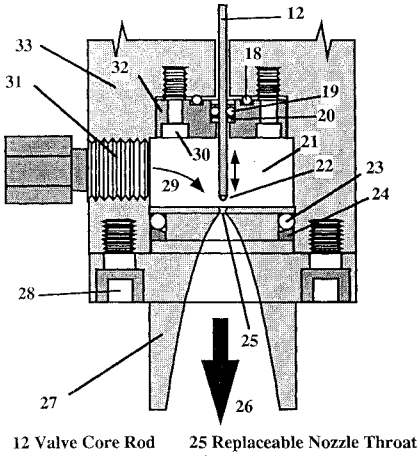

Fig. 2 Detail of the high pressure valve cavity of the HSILS.

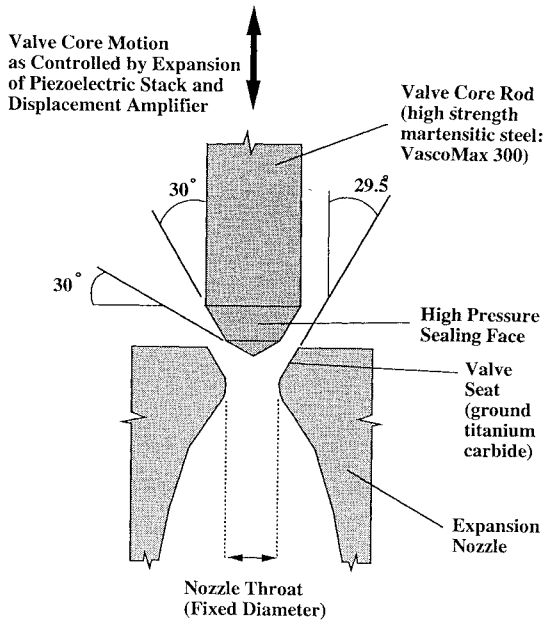

Fig. 3 High-pressure variable mass flow valve seat.

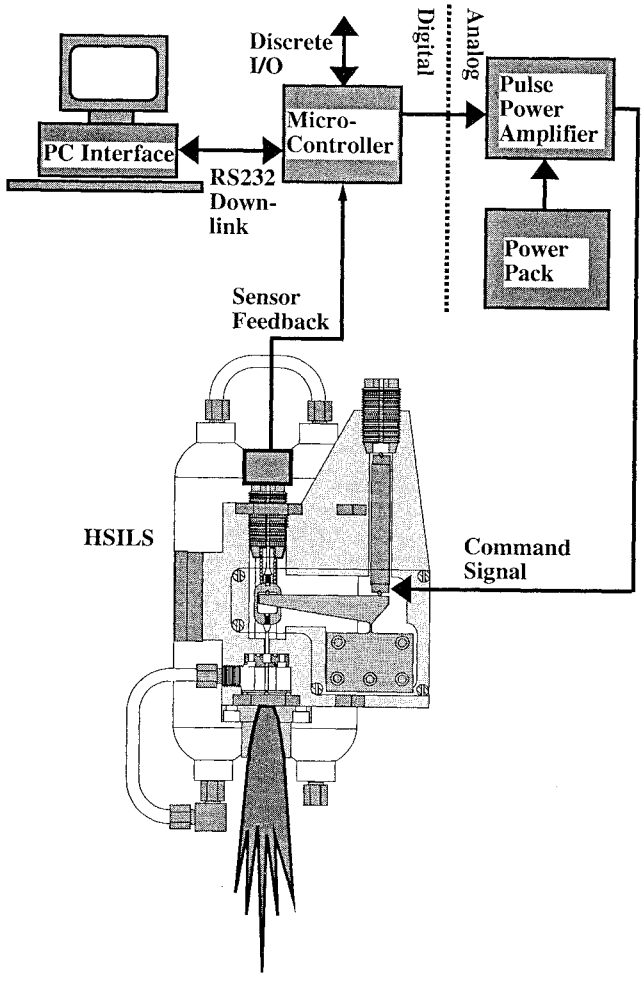

Fig. 4 HSILS control system block diagram.

blocked force curves for any piezoelectric element, with one curve for each unique drive voltage. The relationship between force and displacement at any given drive voltage is typically linear. However, the force (y-axis) intercept may not be linearly related to the drive voltage, hence two separate equations of state are required to characterize the stack.

The performance characteristics described above and in Fig. 5 can be considered representative of the best available today for commercial grade piezoelectric, as well as magnetostrictive, materials.[10–14] However, even with a relatively long, hybrid stack, 0.2% strain is insufficient for operation of an effective rocket engine feed-line valve. To be practicable, a strain of approximately 1–2% would be required for direct axial operation of a thruster capable of producing a force amplitude sufficient for active control purposes.

Accordingly, the design employs a specially designed mechanical displacement amplifier that produces as its output a displacement opposite in direction to the expansion (or contraction) of the piezoelectric stack and 12 times larger than the absolute magnitude of the piezoelectric stack displacement. The amplifier consists of a stiff eccentric titanium anvil (Fig. 1), which is monolithically milled

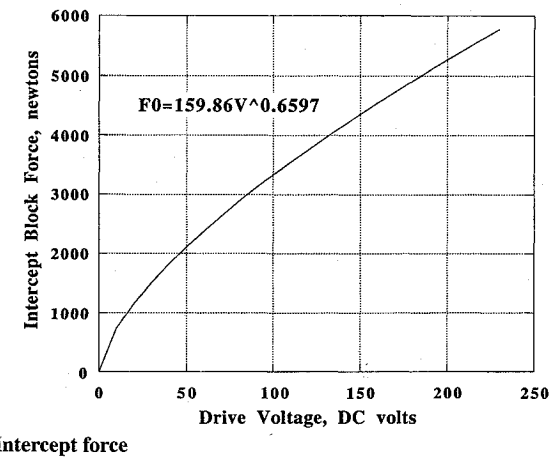

a) Intercept force

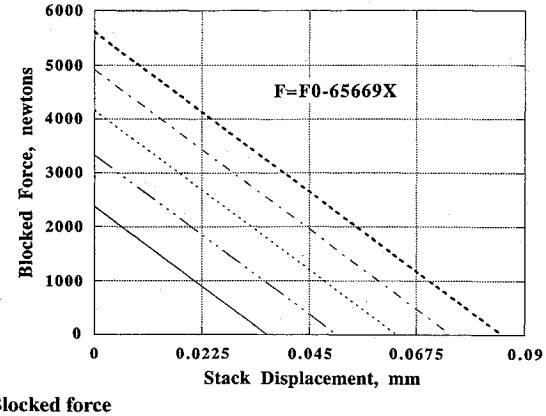

b) Blocked force

Fig. 5 Piezoelectric characteristics for stack used in HSILS.

from a common base block that also forms the support means. The anvil is connected to the support means by a wire EDM-milled hinge that is integral to both the anvil and the support means and comprises a structural element that provides neglible resistance to rotation about an axis perpendicular to the plane of the anvil. The hinge is also designed to provide stiff resistance to displacements and rotations perpendicular to its rotational axis. The intent is to provide, as nearly as practicable, a rigid lever, the fulcrum of which is provided by the hinge.

The piezoelectric stack is provided with special low-friction, high-strength spherical sapphire bearings at both ends, which ensure axial transmission of force as the stack expands under increasing voltage. One such bearing forms an interface with an adjustable, threaded nut that serves as a moveable reaction surface within a housing. The bearing means at the output end of the piezoelectric stack forms an interface with the short side of the lever/anvil of the displacement amplifier. Because nearly all commercial piezoelectric stacks come with parallel milled end faces, conical bearing seats were fabricated from hardcoated aluminum and bonded to the stack ends using strain gauge glue.

The output of the displacement amplifier is connected to a valve core by a similar low-friction, high-strength sapphire bearing in such a way that as the piezoelectric stack expands under increasing applied voltage, the valve core lifts off its corresponding valve seat and permits high-pressure gas and/or propellant to flow. To achieve continuous control, however, the valve core must be capable of being returned to the closed position under positive control. This is achieved by use of a suitable adjustable force compression spring means that maintains the valve in a normally closed position. The spring force is designed to ensure that the closing acceleration of the valve core is capable of matching the amplified contraction acceleration of the piezoelectric stack in such a manner as to maintain all of the bearings in a state of continuous compression.

The valve core is constrained to move in a linear fashion by various guides and seals that additionally serve to prevent buckling of the core rod during the application of compressive loads and to damp out unwanted vibrations. The valve seal is achieved by means of a metal-to-metal contact between the end of the valve core, which is tapered at an angle (59 deg inclusive) and mates to the valve seat, which is also tapered but with an angle (60 deg inclusive) slightly larger than that for the valve core (Fig. 3).

In the prototype thruster, the valve seat is integral with the throat of an expansion nozzle. A chamber on the interior side of the valve seat is in communication with a high-pressure reservoir of gas (e.g., nitrogen). The expansion of this gas through the nozzle as the valve core is raised from and lowered to the closed position creates thrust directly proportional to the displacement of the valve core, and therefore directly proportional to the control signal (voltage-time history) used to drive the piezoelectric stack. The actual response speed (as manifested in the delay time) between a step change in control voltage to the piezoelectric stack and the corresponding change in thrust level at the nozzle are determined by the response time of the piezoelectric stack and the propagation speed of the resulting displacement disturbance through the mechanism to the valve tip. Through structural dynamics calculations, this response speed can be shown to be substantially better than for any of the aforementioned alternative valve technologies.

Control System

Two primary elements, an embedded microcontroller and a pulse power supply, comprised the electronics control system for the thruster. The unit handled one analog strain-gauge-type input, four discrete inputs, one analog output, and four discrete outputs. Onboard software, written in C and Assembly, allowed for downloading of arbitrary voltage-time drive histories from a remote PC followed by either local or remote execution of the profile by the actuator. Complete details, including schematics and software, are presented in Ref. 8.

Performance Parameters

For purposes of comparison with alternative technologies, several parameters were defined to characterize the drive pulse fed to the thruster and the subsequent thruster response. These are shown graphically in Fig. 6. They define various command and response terms associated with a reaction control system in which a half-square wave command pulse is issued. Although arbitrary drive waveforms are possible with this system, the results reported here are constrained to the response of the thruster when subjected to half-square wave drive pulses with varying amplitude and duration.

There is usually a lag time associated with both the rising and falling edges of the thrust pulse, relative to the rising and falling edges of the command signal. In a real reaction control system, there will also be oscillations associated with the rising and falling

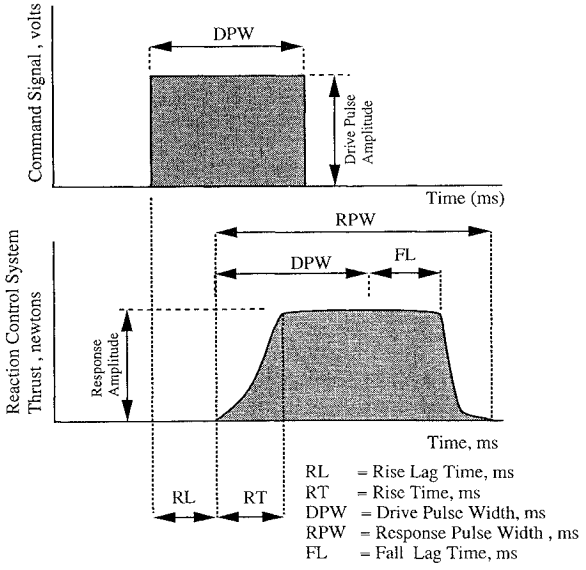

Fig. 6 Command and response transient performance definitions.

edges of the thrust pulse. The rise lag (RL in Fig. 6) is defined as the elapsed time from the leading edge of the drive (or control) pulse to the initiation of measurable thrust. This is a measure of the electromechanical efficiency of the actuator. Rise lag time is associated with mechanical response times of, for example, electrostrictive elements (piezoelectric stacks); wave propagation through connecting elements of a displacement amplifier; the presence of various sources of friction and viscous damping; and reaction times for fuel constituents (if a bipropellant is used instead of a compressed gas).

The response pulse width (RPW in Fig. 6) is defined as the base-to-base time of the response thrust profile, which equals the elapsed time from thrust initiation to thrust termination for an actuator responding to the minimum amplitude half-square wave command signal required to initiate measurable thrust. The RPW is a useful measure of the absolute shortest impulse that can be produced by a reaction control system.

If one views rise lag as electromechanical propagation delay, then one might expect the response pulse to terminate at a time interval equal to the drive pulse width (DPW in Fig. 6) following initiation of measurable thrust from the actuator. In actual fact, this proves not to be the case. The difference in elapsed time from initiation of measurable thrust to the point at which thrust commences a marked decrease minus the DPW constitutes the parameter known as *fall lag* (FL in Fig. 6). For inductive-type systems (e.g., solenoid coils) this results from delays in the collapse of the magnetic field. It can also result from mechanical delays caused by having to overcome static friction in seals.

Hardware

A laboratory prototype HSILS unit, shown in Figs. 7 and 8, was constructed in order to test the feasibility of the concept and to determine some of its operating characteristics and limitations. Complete hardware details are described in Ref. 8. The device shown in Fig. 7 comprises the entire HSILS unit, which can be operated in stand-alone mode once the compressed gas and capacitor storages banks are charged. No great efforts were undertaken to minimize space and weight. The large box to the left of the thruster unit was used to house the microcontroller, capacitor discharge banks, and power amplifiers. The smaller boxes comprised signal conditioning and power supplies for acoustic and pressure sensors used to measure pulse width and thrust.

The HSILS thruster includes a 41.4 MPA dry nitrogen charging line connected to the onboard gas accumulator bank. Once the accumulators were charged, this line could be disconnected and several tests conducted before recharging became necessary. The high-voltage (0–300 V) output of the pulse power supply was connected to the piezoelectric stack via a jacketed BNC-type connecter, shown at midheight on the left of the unit. Fig. 8 is a view of the internal working components of the HSILS, including the titanium displacement amplifier, the piezoelectric stack and its associated sapphire spherical end bearings, and the connector/pivot mechanism, which links the displacement amplifier to the valve core rod and its associated spring return system.

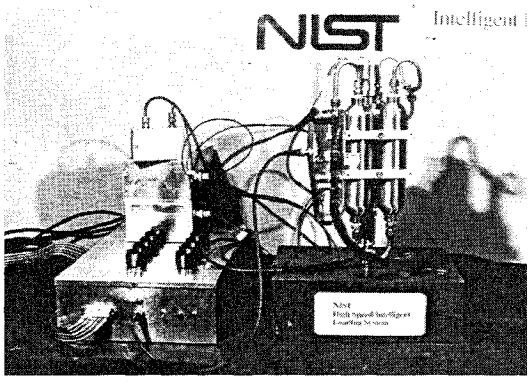

Fig. 7 HSILS microcontroller and pulse power supply (left) and HSILS cold gas thruster unit with attached high-pressure accumulators (right).

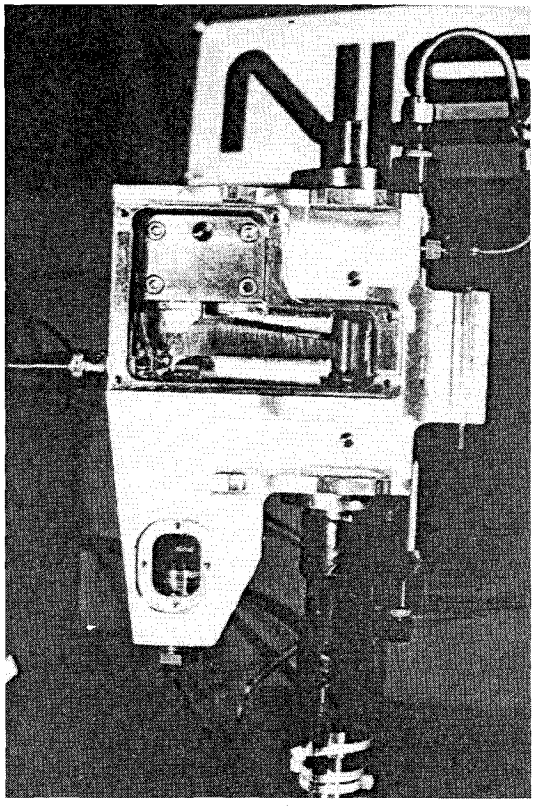

Fig. 8 Close-up sideview of HSILS thruster unit showing piezoelectric stack, titanium displacement amplifier, and valve core yolk.

In addition to the piezoelectric-driven unit, a simple solenoid-based compressed gas thruster was constructed to serve as a control experiment. This was used to provide companion data that would be representative of traditional reaction control system thrusters.

Sensors

It was initially thought that a responsive load cell could be used to measure the thrust output of both the HSILS and RCS (solenoid) thrusters. However, and as was subsequently ascertained independently by Hallauer et al.,[9] this led to unwanted high-level noise in the response signal that represented the vibration of the structural system consisting of the force actuator and the load cell. It was shown that this effect became worse as efforts were made to make the load cell more sensitive (and therefore more flexible). Hallauer et al.[9] ultimately made use of dynamic piezoelectric-based load cells, which were by nature quite stiff. However, at the time of testing of the HSILS unit, piezoelectric cells were not available to the author, and alternative methods were developed for determining the minimum pulse width resolution and to measure qualitatively the amplitude (thrust) response of the two candidate actuators.

The first sensor consisted of a commonly available PC Mount condenser microphone element. The actual unit had a 2.0–10 V operating range; 1.0 mA maximum current drain; 40 dB minimum signal-to-noise ratio; -65 ± 4 dB sensitivity over the range of 20 to 20 khz; and an output impedance of 1k ohms. This element was placed at the exhaust lip of the actuator nozzle. This meant that there was an inherent delay from the time the valve core first lifted off the seat until the sensor detected perceptible thrust of approximately 75 μs, owing to the propagation speed of sound in air. This was included in the recorded rise-lag times.

Although the acoustic sensor provided an accurate means for determining pulse width, it was incapable of providing quantitative thrust measurement data (qualitatively, the noise amplitude did seem to be proportional to thrust, but there was no reliable means of calibrating this). Given the low levels of anticipated thrust, an approach was developed that employed a vented chamber attached to the end of the nozzle. A Keller-PSI-PA-9, 10-bar semiconductor absolute pressure transducer was mounted on the face of the vented

chamber opposite the actuator nozzle. Thrust was then approximately measured by means of equivalent static exhaust pressure. It was realized at the outset that higher thrust levels would lead to greater turbulence, and therefore greater scatter in the resulting data. However, the results were shown to be repeatable and proportional to the exhaust pressure, and therefore they served as a useful crude measurement of thrust. In this respect, the reader should remember that the purpose of these initial tests was to demonstrate the concept of variable thrust control, not to calibrate the unit.

Pulse-Width Tests

Pulse-width tests for each type of actuator were conducted using the following procedure.

1) Position the acoustic sensor and charge the gas accumulator and power capacitors.

2) Enter a drive pulse command of the form "P XXX YYY." This caused the onboard microcontroller to execute a power discharge to the actuator in the form of a half square wave of width "XXX" microseconds and having a peak (plateau) amplitude of "YYY" volts, dc.

3) Using a two-channel digital signal analyzer, acquire data from the acoustic sensor and drive pulse voltage.

4) Evaluate drive pulse width, drive pulse amplitude, response rise lag, response pulse width, and response fall lag.

Tests of this sort were conducted for both the RCS (solenoid) and HSILS (piezo) systems. All tests were begun with drive pulse widths of approximately 100 ms. This value was then gradually decreased until the threshold actuator pulse was achieved. Drive pulse widths below this value failed to open the valve. Typical limiting repeatable pulse-width responses are shown in Figs. 9 and 10 for the RCS and HSILS systems, respectively.

For the RCS thruster, it was observed that the correlation between the drive and response pulse widths began to degrade for drive pulse

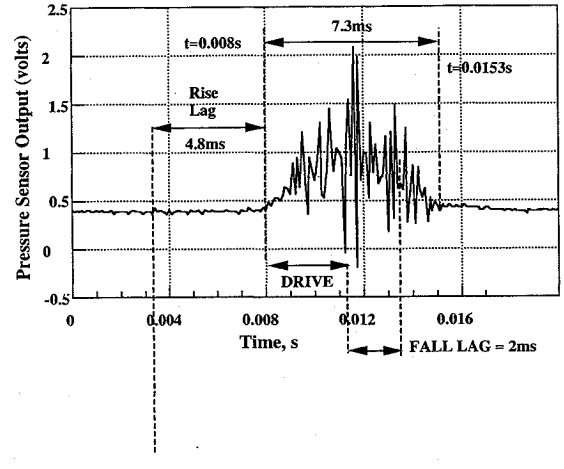

a)

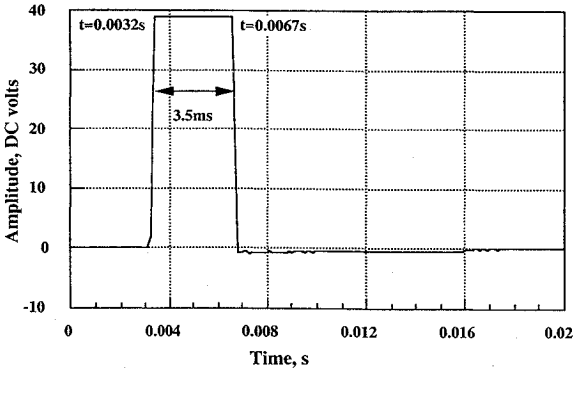

b)

Fig. 9 Limiting pulse-width response for solenoid-based thruster (top) and the drive pulse used to produce the actuator response (bottom).

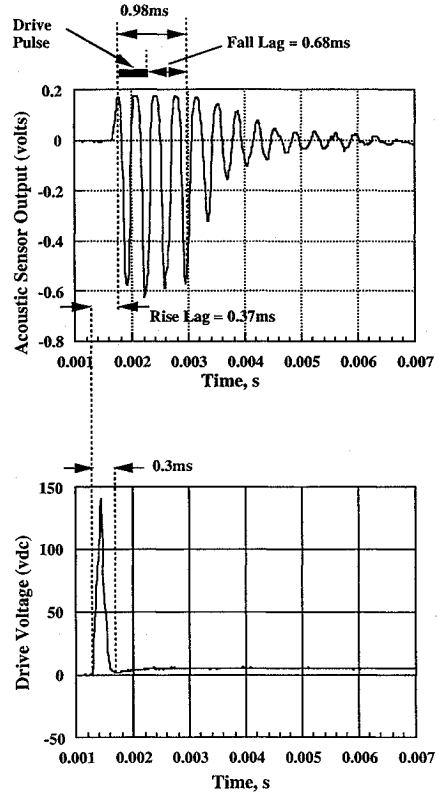

Fig. 10 Limiting pulse-width response for the HSILS prototype (top) and the drive pulse used to produce the actuator response (bottom).

widths of less than about 10 ms. That is to say, for example, that a 0.0036 s drive pulse produces a 0.0301 s response, not a 0.0036 s response. This may be interpreted as approaching the minimum "full-on" pulse width, which comprises the time to energize the inductive solenoid coil, for the magnetic core to lift-off and compress the return spring, and for the field to collapse and the compression spring to return the core to its closed position. At some point, a drive pulse becomes short enough to produce a "ballistic" trajectory from the valve core; that is, the energy is insufficient to pull the valve core away from the exhaust orifice to its fully retracted position, but it is sufficient to just cause lift-off. This type of response can be seen in Fig. 9 and can be considered the minimum achievable pulse for the RCS thruster tested.

Fig. 10 presents the corresponding minimum repeatable pulse width for the HSILS prototype. It is particularly noteworthy that the entire pulse width is approximately 1 ms. As a result the nature of the acoustic noise that is superimposed on the signal is more evident than for the RCS tests. It has been determined from frequency analysis that the noise has a strong dominant frequency of approximately 4 khz. This corresponds closely to the characteristic acoustic resonant frequency of the expansion nozzle. Because the nozzle continues to vibrate for a small period of time after ceasation of the delivery of gas a resonant decay can be expected (centered about the x-axis) at the tailend of each pulse. This was observed in most of the shorter HSILS response pulse records. In all such cases, there was a dramatic reduction in overall amplitude at the point at which the valve closes. This point corresponds to the termination of thrust.

There is a limiting drive pulse amplitude, below which measurable thrust is not produced by the HSILS. The limiting drive voltage appears to be approximately 85 volts. That such a threshold drive voltage exists can be understood by considering the blocked force diagram for the piezoelectric stack presented earlier. The stack must initially generate a force necessary to cause the valve core to lift off the valve seat by an amount sufficient to create measurable thrust. However, such motion is prevented by the return spring at the end of the displacement amplifier. The force necessary for lift-off is, therefore, the return spring precompression times the amplification factor for the displacement amplifier, which in the case of the HSILS

prototype unit was 12. Because experimental data indicated that an 85-V amplitude was required to initiate measurable thrust, we can calculate that the valve core displacement at that time was 0.007 mm.

Amplitude Control Tests

The ability to create arbitrary output thrust profiles implicitly requires the ability to vary the thrust amplitude. Therefore, a series of tests were conducted on both the HSILS and RCS (solenoid) units to determine their steady-state response to various amplitude control voltages. In the results shown in Figs. 11 and 12 the thrust level was determined as previously described in terms of equivalent static exhaust pressure times the sensing element area. These values, therefore, represent relative, not absolute, thrust. The test protocol was as follows.

1) Position an absolute pressure sensor in a vented chamber over the nozzle, and charge the gas accumulator and power capacitors.

2) Apply continuous dc voltage to the respective actuators for a period of approximately 0.5 s.

3) Using a two-channel digital signal analyzer, acquire data from the acoustic sensor and the drive pulse voltage.

4) Determine the mean thrust from the average output signal after attaining steady-state response.

Figure 11 shows the amplitude response characteristics for the RCS (solenoid) actuator. This clearly indicates the presence of a threshold drive voltage of approximately 17 V. After this threshold has been reached, the level of thrust is shown to be constant with increasing voltage. This type of performance is the primary impediment to using solenoid-based actuators for variable thrust control. Other limitations, in the form of rise and fall lag times and minimum pulse width, are discussed in detail below.

Figure 12 shows the amplitude response characteristics for the HSILS prototype. This indicates linear amplitude response with increasing drive voltage. There is increasing scatter in the data beyond a drive voltage of approximately 180 V, presumably caused by turbulence, although the trend (increasing thrust with increasing drive voltage) is still preserved. A regression equation relating empirical thrust to drive voltage is given. The manufacturer's maximum recommended drive voltage for the piezoelectric stack used in these tests is 300 V. However, for reasons of conservatism, the amplitude tests were limited to drive voltages less than 240 V. At higher voltages there exists the potential for shorting (arc over) between the stack elements and the subsequent loss of either a stack block subassembly or the entire stack.

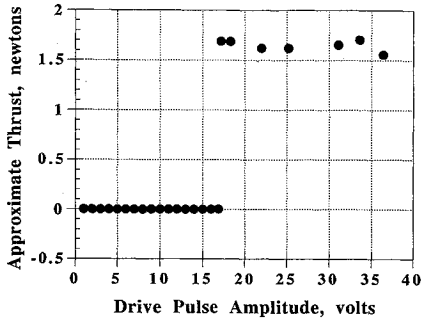

Fig. 11 Approximate amplitude (thrust) response characteristics for the solenoid-based thruster.

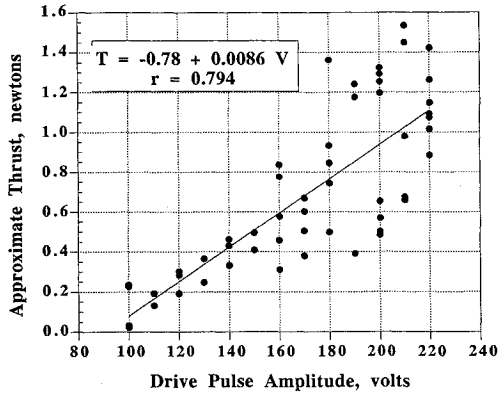

Fig. 12 Approximate amplitude (thrust) response characteristics for the HSILS prototype thruster.

Discussion

Table 1 presents for comparison several performance parameters that can be derived from the minimum repeatable pulses for the RCS and HSILS prototypes.

All of the response variables for the RCS actuator compare favorably with data presented by Hallauer et al.[9] for a similar solenoid valve from a different manufacturer. The right-most column in Table 1 gives the ratios of the RCS response to those measured for the HSILS prototype. From these it can be seen that the HSILS actuator clearly outperforms the solenoid actuator on all counts. Pulse width control and rise lag for the HSILS are nearly an order of magnitude faster than for the solenoid actuator.

The lowest performance improvement for the HSILS unit is the fall lag, which is only three times faster than for the solenoid and four times longer than the HSILS rise lag. This may be attributable to differences in the loading and unloading mechanisms used in the HSILS. Initial expansion of the piezoelectric stack occurs very rapidly (approximately 10 μs to full extension), and the stack is capable of generating extremely high levels of force (upwards of 8000 N) at low initial displacements. On the other hand, the return force needed to close the valve is provided by a compression spring with a constant force level of approximately 200 N. Given the high degree of damping in the system provided by the high-pressure valve core seals, this difference in force levels could account for the increased fall lag. Methods for improving this response might include low-friction seals and a higher return spring force or, alternatively, a parallel piezoelectric stack used solely for closing the valve.

A number of parameter studies were conducted, which included correlation plots of response pulse width vs drive pulse width; response pulse width vs drive pulse energy; response rise lag vs drive pulse amplitude; response fall lag vs drive pulse energy; and response fall lag vs drive vs pulse width. These are presented in Figs. 13 and 14 for the RCS and HSILS actuators, respectively.

RCS (Solenoid) Results

Figure 13a indicates that for longer drive pulse widths, there is a reasonable degree of correlation between the response and the drive pulse width. This correlation appears to break down for drive pulse widths of less than 10 ms.

Figure 13b shows the relationship between RCS response pulse width and drive pulse energy. For this comparison, the active energy dissipation in the drive pulse was calculated as follows for the resistive-inductive load provided by the solenoid coil when driven by a constant current pulse power supply:

$$E_{RCS} = \sum_{i=1}^{m-1} \left[\frac{V(i+1) + V(i)}{2R} \right] [t(i+1) - t(i)]i$$

As can be seen in Fig. 13b there seems to be a power–law relationship between solenoid response pulse width and the amount of energy provided to the coil. This is a somewhat intuitive observation because power must be continuously supplied to the coil to sustain the magnetic field that causes the valve to remain open once the initial opening threshold energy content has been reached. The same

Table 1 Comparison of RCS and HSILS response parameters

Parameter	RCS, solenoid	HSILS, piezoelectric	RCS/HSILS
Drive pulse width, s	0.0035	0.0003	11.67
Response rise lag, s	0.0048	0.00037	12.97
Response pulse width, s	0.0073	0.00098	7.45
Response fall lag, s	0.002	0.00068	2.94

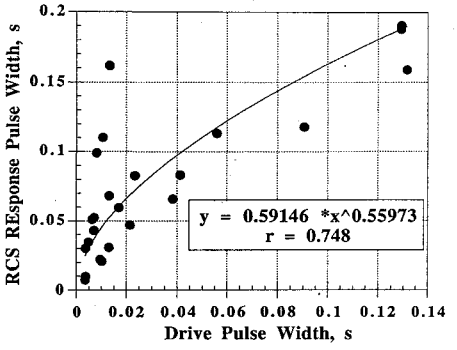

a) RCS response pulse width vs drive pulse width

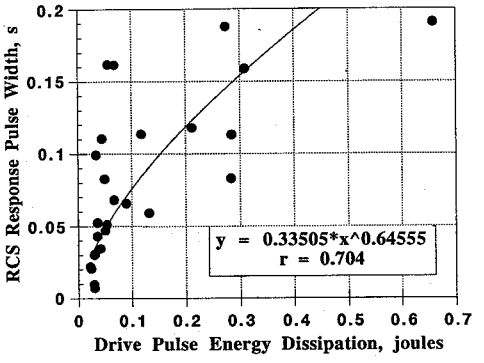

b) RCS response pulse width vs drive pulse active energy dissipation

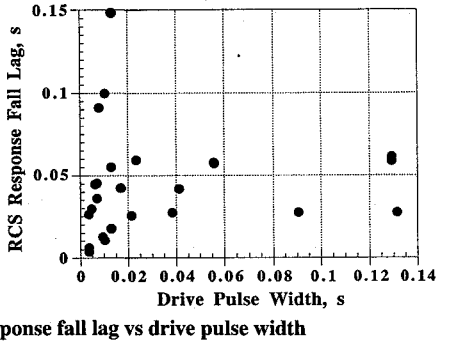

c) RCS response fall lag vs drive pulse width

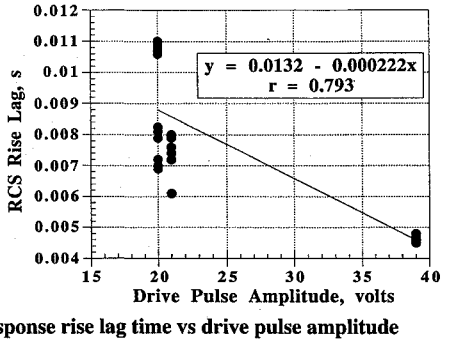

d) RCS response rise lag time vs drive pulse amplitude

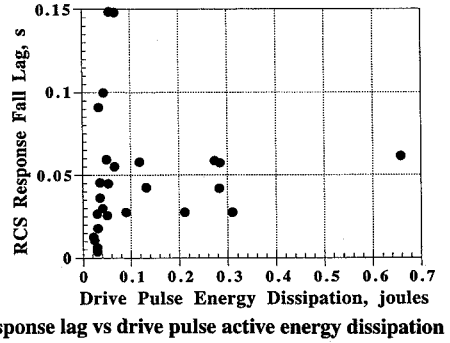

e) RCS response lag vs drive pulse active energy dissipation

Fig. 13 Typical solenoid-based thruster response characteristics.

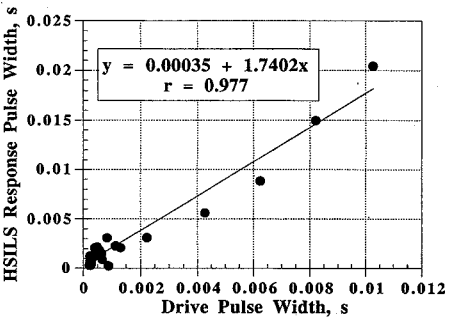

a) HSILS response pulse width vs drive pulse width

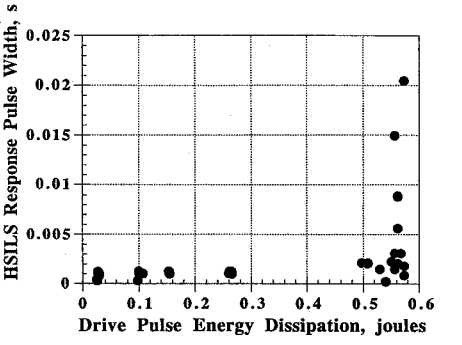

b) HSILS response pulse width vs drive pulse active energy dissipation

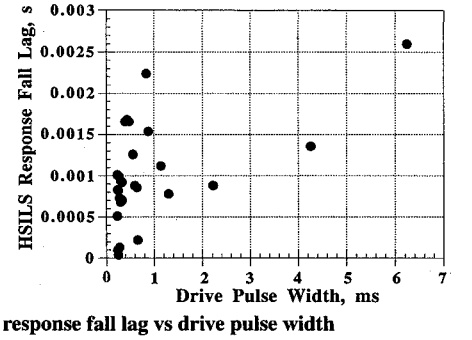

c) HSILS response fall lag vs drive pulse width

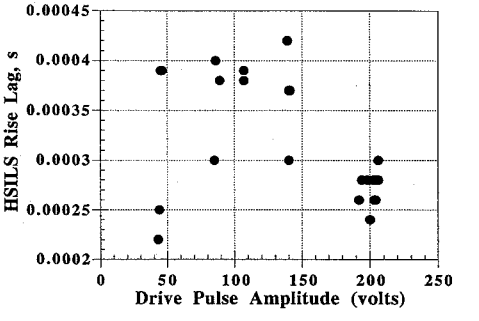

d) HSILS response rise lag time vs drive pulse amplitude

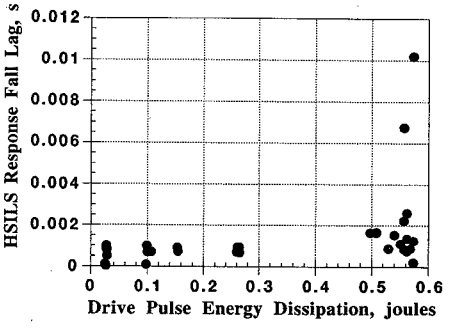

e) HSILS response fall lag vs drive pulse active energy dissipation

Fig. 14 Typical HSILS prototype thruster response characteristics.

cannot be said for RCS fall lag (Fig. 13c), which shows no correlation to drive pulse energy nor to drive pulse width (Fig. 13d). RCS rise lag, on the other hand, does seem to be correlated to the drive pulse amplitude (maximum drive voltage), with shorter rise lag (5 vs. 9 ms) corresponding to the higher of the two voltage plateaus employed in these tests (39 and 21 V, respectively).

HSILS Results

A similar set of correlation plots for the HSILS prototype is shown in Fig. 14. Here it can be seen (Fig. 14a) that, unlike the RCS actuator, there is a good linear correlation ($R^2 = 95.5\%$) between the HSILS response pulse width and the drive pulse width.

Unlike the RCS unit, there is no correlation between HSILS response pulse width and drive pulse energy (Fig. 14b). For the case of a capacitive load (for which a piezoelectric stack is a good emulator) driven by a constant current pulse power supply the active energy dissipation is given by:

$$E_{HSILS} = \tfrac{1}{2} C V_{\text{peak}}^2$$

Once a plateau level has been reached in the drive pulse, the piezoelectric stack will remain extended (and will, therefore, hold the valve open) with no expenditure of energy, as evidenced by the grouping of points at approximately 0.6 J in Fig. 14c. The ability of the piezoelectric stack to store energy also means that the energy must be removed in order to reduce the thrust level. It was for this reason that the pulse power supply employed parallel high-power transistor banks: one for charging (extending), and one for discharging (contracting) the stack. Similar data to that shown in Fig. 14 could have been collected for any of the lower energy content pulses. The density of data at 0.6 J is a result of most of the pulse-width tests being conducted with a 200 V amplitude drive pulse. A similar lack of correlation exists between response fall lag and dissipated energy, as shown in Fig. 14d. Nor does there seem to be any correlation between response fall lag and drive pulse width.

Fig. 14d also indicates that there is no relationship between the drive pulse amplitude and the response rise lag. The data spread in rise lag for the HSILS unit are on the order of 0.2 ms and do not seem to be a function of any drive pulse characteristics. The HSILS fall lag, on the other hand, (Figs. 14d and 14e), shows local data spread of as much as 1.5 ms, particularly for drive pulse widths in excess of 0.5 ms. These may be related to the valve momentarily sticking in the open position following termination of the drive pulse. This would most likely be a result of differences in kinetic and static friction at the location where the valve core rod penetrates the high pressure chamber inboard of the exhaust nozzle throat. Along this section are several o-rings, backup rings, and a guide tube for the valve core that exhibit a high level of damping.

It is more likely that fall lag and fall lag variances for the HSILS will be greater than rise lag (and its associated variances), because the return spring used in the present HSILS prototype is incapable of developing the instantaneous high initial loads that the piezoelectric stack can upon initial valve opening. During initial cracking of the valve, as with closing from a stable open position, static friction at the high-pressure seals will be greater than kinetic friction. The longer it takes to overcome the transition from static to kinetic friction, the greater will be the expected lag and the level of variance. Because during valve opening the stack is able to adaptively increase the opening force, it can proceed through this friction transition faster, leading to lower variance in rise lag.

Amplitude Control Using HSILS

As shown in Fig. 12, there exists a linear relationship between output thrust and drive voltage for the HSILS prototype. The actual thrust levels involved were low. The calculated peak thrust, based on standard nozzle theory,[15] was on the order of 1–2 N for an accumulator pressure of 5.5 MPa.

Supplementary testing was done at operating pressures as high as 41 MPa with a commensurate improvement in thrust amplitude (i.e., in the calculated range of 7–15 N). At these higher thrust levels, there were occasional instances where the valve did not close perfectly, as evidenced by a residual gas leak. This occurred more frequently for the initial valve seat configuration in which the expansion nozzle and valve seat were integrally machined from a rod of 304 stainless steel. The valve core rod was machined from hardened drill rod (yield strength 1884 MPa, hardness 15N-86). After several thousand test firings, it was noted that the 304 stainless steel at the valve seat developed a localized spall due to impact fatigue (with subsequent detectable blow-by upon closing of the valve).

Ultimately, the valve-seat/nozzle-throat segment of the expansion nozzle was redesigned as a replaceable unit. Two new materials were used for the replaceable valve seat: VascoMax 300 [yield strength 2760 MPa, hardness 92-HR15N (approx. HRC-65)] and Ferrotic alloy (yield strength 3000 MPa MPa, hardness 2470-HK). Vascomax 300 is a commercial maraging steel developed by Vanadium Alloy Steel Company with a yield strength of 300 ksi, 5–8% elongation-to-fracture, and little work-hardening capacity. It has a toughness of about 45 ksi-sqrt (in.) (Ferro-Tic CS-40, manufactured by Chromalloy American Corp. of West Nyack, NY consists of 45% by volume TiC in a matrix of high chromium, ferritic stainless steel. The matrix is heat treatable to various strength and toughness levels.) Of these the Ferrotic seat performed best, and there was no subsequent marring of the valve seat surface. (Certain trade names and company products are mentioned in the text or identified in an illustration in order to specify the experimental procedure and equipment used adequately. In no case does such identification imply recommendation or endorsement by the National Institute of Standards and Technology, nor does it imply that the products are necessarily optimal for the purpose.) However, after several hundred additional firings, it was discovered that the blow-by problem had reappeared. This time a small striated patch (approx 0.05 mm^2) appeared on the valve core rod sealing surface at the valve tip. Although the problem was resolvable in the laboratory by simply replacing the valve core rod, further research is waranted into the design of this detail of the HSILS, particularly for higher operating pressures.

Damping Effects

Laboratory measurements of viscous damping yielded an estimate of the HSILS internal damping ratio of 388% of critical. The limiting repeatable HSILS response shown in Fig. 10 indicates negligible amplitude oscillation upon reaching the full-open position and likewise negligible amplitude oscillation following valve closing. The vibrations that are superimposed on the steady-state response and that decay following closing of the valve are, as previously reported, acoustic ringing of the exhaust nozzle. Although the high-pressure seals that isolate the valve core drive mechanism from the pressurized gas chamber are likely a strong factor in determining the limiting pulse-width resolution (due to increased fall lag), they are both necessary to the isolation of the pressurized portion of the operational device, as well as to eliminate bounce as the valve closes. Future enhancements to the device will necessarily deal with the tradeoffs inherent in eliminating valve core bounce while minimizing response lag times.

Conclusions

A working laboratory prototype HSILS was developed and tested in side-by-side comparisons with traditional solenoid-based reaction control technology. The HSILS concept employed a mechanically amplified piezoelectric stack as the active valve element in a cold gas thruster as opposed to an electro-magnetically operated valve core. The HSILS unit exhibited the following levels of performance improvement.

1) Minimum rise lag of 0.37 ms. This value is 13 times faster than for equivalent solenoid-based reaction control systems.

2) Response pulse-width resolution of 0.98 ms. This value is approximately 8 times faster than for an equivalent solenoid-based system.

3) Minimum response fall lag of 0.68 ms. This value is approximately 3 times faster than for an equivalent solenoid-based system.

Linear amplitude control was achieved beyond a threshold drive level of 80 vdc through the limiting level of 240 vdc used in the tests. Solenoid-based technology was shown to have binary thrust behavior (either off or full-on). The HSILS laboratory prototype was capable of delivering a peak thrust of approximately 15 N at

an accumulator pressure of 41 MPa. Scaling of the HSILS unit to achieve larger maximum thrust seems feasible without significant penalties to the performance characteristics determined in this study.

The HSILS system was controlled by a dedicated onboard microcontroller and pulse power system, which, after being charged, could be operated in a stand-alone mode. Compressed nitrogen accumulators were an integral part of the laboratory prototype, so that the entire package could be attached to a structural system to serve either as a remote, independent active control or system identification node.

Several areas for future improvement and research were identified. Fall lag times were disproportionately high with respect to the observed rise lag times. This was traced to the differences in the opening and closing mechanisms used in the present HSILS design. Currently a fast-acting piezoelectric stack is used for valve opening and a preloaded compression spring for valve closing. The former is capable of dynamically increasing its force level, particularly at small displacements. The resistance to valve opening and closing arises from high-pressure seals that separate the pressurized section (the valve seat area) from the unpressurized core actuator mechanism. Additional problems were noted at the valve seat where high-strength, high-hardness valve elements had to mate precisely, and repeatedly, at closing velocities of 4–5 m/s. Reasonable sealing performance was obtained by using a 2000 MPa maraging steel valve core rod and an EDM milled and polished valve seat fabricated from a ferritic titanium carbide alloy. Visible warping of the valve core rod, which was quite slender, was observed following several thousand test firings, as was minor galling on the valve core rod tip.

References

[1]Carasso, A. S., and Simiu, E., "Estimation of Dynamic Green's Functions for Large Space Structures by Pulse Probing and Deconvolution," *Computational Mechanics '88*, Vol. 2, Springer–Verlag, New York, 1988, pp. 44.vii.1–44.vii.4.

[2]Carasso, A. S., and Simiu, E., "Dynamic Characterization of Structures by Pulse Probing and Deconvolution, AIAA Paper 88-2230, April 1988.

[3]Carasso, A. S., and Simiu, E., "Identification of Dynamic Green's Functions in Structural Networks," *ALAA Journal*, Vol. 27, No. 4, 1989, pp. 492–499.

[4]Simiu, E., and Cook, G. R., "Impulse Response Functions for Elastic Structures with Rigid-Body Degrees of Freedom," *Journal of Sound and Vibration*, Vol. 135, No. 2, 1989, pp. 275–288.

[5]Carasso, A. S., "Probe Waveforms and the Reconstruction of Structural Dynamic Green's Functions," *AIAA Journal*, Vol. 29, No. 1, 1991, pp. 114–118.

[6]Belvin, W. K., and Edighoffer, H. H., "Dynamic Analysis and Experiment Methods for a Generic Space Station Model," AIAA Paper 86-0838, May 1986.

[7]Stone, W. C., "High Speed, Amplitude Variable Thrust Control," Patent Pending, U.S. Patent and Trademark Office, Crystal City, VA, Ser. No. 07/873,020, Oct. 1993.

[8]Stone, W. C., "Development of a Fast-Response Variable-Amplitude Programmable Reaction Control System," NISTIR-5118, National Institute of Standards and Technology, Gaithersburg, MD, Jan. 1993, p. 246.

[9]Hallauer, W. L., Lamberson, S. E., and Baer, C. A., "Active Vibration Damping of a Planar Truss Using Air-Jet Thrusters," *Experimental Mechanics*, Vol. 31, No. 3, 1991, pp. 189–196.

[10]Randeraat, J. V., and Setterington, R. E. (eds.), *Piezoelectric Ceramics*, 2nd ed., Mullard Limited, London, 1974, p. 211.

[11]Takahashi, S., "Recent Developments in Multilayer Piezoelectric Ceramic Actuators and Their Applications," *Ferroelectrics*, Vol. 91, March 1989, pp. 293–302.

[12]Hiratsuka, H., Kawasaki, K., and Miyo, Y., "Flow-Control Type Piezoelectric Element Valve," U.S. Patent 5,029,610 U.S. Commissioner of Patents and Trademarks, Crystal City, VA, July 1991.

[13]Guide to Modern Piezoelectric Ceramics," Morgan Matroc, Electro Ceramics Division, Bedford, OH, March 1993.

[14]Lacheisserie, E., *Magnetostriction: Theory and Applications of Magnetoelasticity*, CRC Press, Boca Raton, FL, 1993, p. 408.

[15]Sutton, G. P., *Rocket Propulsion Elements*, 5th ed., Wiley, New York, 1986, p. 361.

J. A. Martin
Associate Editor